Depth estimation of buried objects using wavelet transform and statistical hypothesis testing

A. Burak Yoldemir and Mehmet Sezgin

TÜBİTAK UEKAE, Gebze, Kocaeli, Turkey

ABSTRACT

In the underground inspection problem, signature of a big target at a certain depth may give equivalent information to the signature of a smaller target at shallower depth, unless depth information is not used. This results in a difficulty in the identification process. Therefore, depth information is coming into prominence in the classification step to increase the identification performance. In this study, we propose a burial depth estimation method on GPR data. In our work, discrete wavelet transform is used in the preprocessing step. After this stage, statistical hypothesis tests are utilized to detect the statistical discrepancies in the returning signals at different depth levels.

Keywords: Ground penetrating radar (GPR), buried object identification, depth estimation, discrete wavelet transform, statistical hypothesis testing

1. INTRODUCTION

Ground penetrating radar (GPR) has an enormously wide range of applications, including archaeological investigations, building condition assessment, forensic investigations, planetary exploration and detection of buried mines.[1] This study focuses on depth estimation of buried objects using GPR, with special emphasis on dangerous objects such as landmines. Depth information is of paramount importance for the buried object identification problem. Reason of this phenomenon is that, the target signature is highly affected by the burial depth. The GPR signal returning from a large object buried at a certain depth may be very similar to the signal returning from a smaller object buried at a shallower depth. Hence, depth information is crucial for buried object identification step.

To the best of our knowledge, there is not much work on depth estimation of buried objects using GPR in the literature. In a previous study by Ho *et al.*,[2] a depth estimation method is proposed, which relies on correlating a slice in down-track and a slice in cross-track for different depth levels. In this study, we propose a novel burial depth estimation method on GPR data based on hypothesis testing. In our work, discrete wavelet transform is used in the preprocessing step. This step consists of getting rid of the ground bounce and other redundancies in the received GPR signal. After this stage, statistical hypothesis tests -which point out the likelihood of an assumption made about a sample-, are utilized to detect the statistical discrepancies in the returning signals at different depth levels. The first level at which such statistical differences occur is marked as the burial depth of the object. It should be noted that, in this study, we assume object detection step is completed, and the proposed depth estimation technique is applied around the alarm locations only.

When the depth information of the buried object is available, it can be used as a feature in the object identification step, which is generally achieved through supervised learning methods. Given the notable dependence of the received GPR signal on the burial depth, this feature can be expected to be one of the features that steer the learning algorithm.

This paper is structured as follows. Section II discusses the problem formulation and presents the proposed methods. Section III gives the results of applying the techniques to a GPR data set, which is collected using a GPR sensor developed at The Scientific and Technological Research Council of Turkey (TÜBİTAK). Conclusion and direction of future work are given in Section IV, which finalizes our discussion.

Further author information: (Send correspondence to A.B.Y.)
A.B.Y.: E-mail: burak.yoldemir@bte.tubitak.gov.tr, Telephone: 90 262 677 2588
M.S.: E-mail: mehmet.sezgin@bte.tubitak.gov.tr, Telephone: 90 262 677 2541

Detection and Sensing of Mines, Explosive Objects, and Obscured Targets XV,
edited by Russell S. Harmon, John H. Holloway Jr., J. Thomas Broach, Proc. of SPIE
Vol. 7664, 76642C · © 2010 SPIE · CCC code: 0277-786X/10/$18 · doi: 10.1117/12.852529

2. PROBLEM FORMULATION AND ALGORITHM

2.1 Data Representation

Let a B-scan be composed of N A-scans, each of which contains M samples. As this study focuses on highlighting the statistical incongruities between different depth levels, we denote each depth bin by $\mathbf{x}_i$, $i = 1, ..., M$. Each $\mathbf{x}_i$ consists of N elements. Fig. 1 shows the convention used in representing the data throughout this paper.

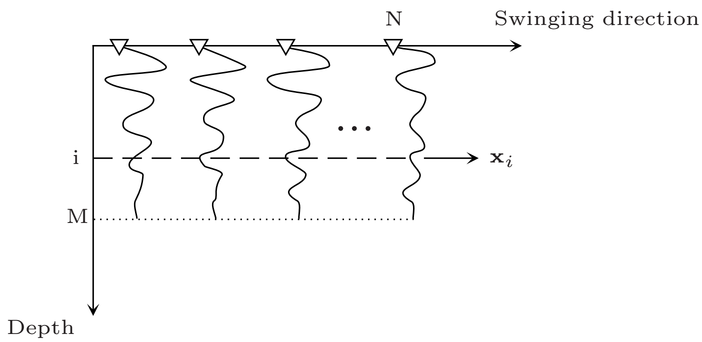

Figure 1. Data representation

For further clarity, a sample B-scan of a VS-50 surrogate mine is given in Fig. 2.

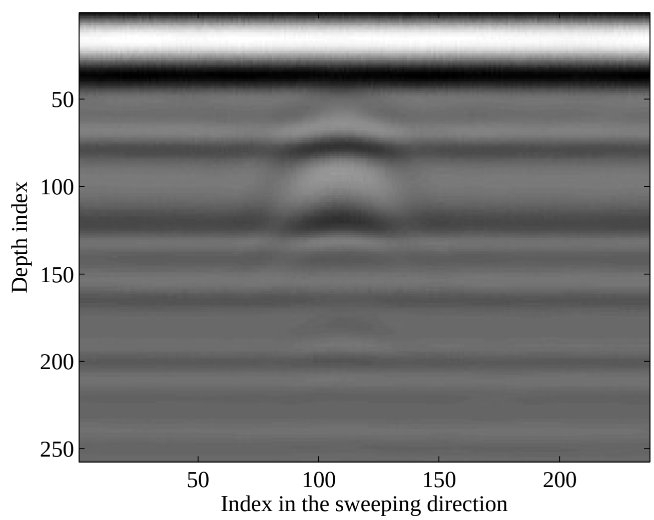

Figure 2. A sample B-scan

2.2 Preprocessing

For removing the clutter inherent in the GPR signals, we apply background subtraction prior to the depth estimation algorithm. For this purpose, an average value of an ensemble of A-scans is subtracted from each A-scan. Obviously, these A-scans are taken at a target-free region.

2.3 Denoising with wavelets

Although background subtraction is a popular technique in GPR signal processing, in general, more advanced denoising strategies are necessary. To this end, we use a wavelet-based denoising technique.[3] This method consists of transforming the data to wavelet domain and canceling out the coefficients that correspond to clutter signatures.

As previous studies suggest, wavelets have a high potential in discriminating Gaussian and non-Gaussian processes.[4,5] Wavelet transform is also capable of providing both time and frequency localization simultaneously. With these motives in mind, we decompose each $\mathbf{x}_i$ to L wavelet levels. We denote the wavelet coefficients corresponding to $\mathbf{x}_i$ by $W_i^j(k)$, where $j = 1, 2, ..., L$ is the decomposition level and $k = 1, 2, ..., K$, where $K = N/2j$. During our experiments, 5th order coiflets are found to be working well for our purposes. A rigorous discussion of the selection of type and order of the wavelets is beyond the scope of this paper.

In this work, noise is assumed to have a Gaussian distribution, and Gaussianity test is applied to each $W_i^j(k)$. We use skewness to test normality, which is the normalized version of the third-order cumulant. For a given $W_i^j(k)$, the normalized skewness is given as

$$S = \frac{E\left\{\left(W_i^j(k)\right)^3\right\}}{\left\{E\left\{\left(W_i^j(k)\right)^2\right\}\right\}^{1.5}}. \tag{1}$$

As we are limited to a limited number of A-scan samples, we need an estimate of skewness. Conventional estimate of skewness is given by[6]

$$\hat{S} = \frac{1}{K}\sum_{k=1}^{K}\left(\frac{W_i^j(k) - \mu}{\sigma}\right)^3 \tag{2}$$

where $\mu = E\left\{W_i^j\right\}$ and $\sigma^2 = E\left\{\left(W_i^j - \mu\right)^2\right\}$. Skewness of a Gaussian process is zero. In our Gaussianity test, we allow a confidence interval for skewness value. This interval can be shown as

$$-\gamma < \hat{S} < \gamma. \tag{3}$$

If the skewness value of wavelet coefficients for a certain decomposition level at a given depth bin falls within these limits, the coefficients at that decomposition level are concluded to have a Gaussian-like distribution, and they are equated to zero. It should be emphasized the wavelet decomposition levels are treated separately, i.e., wavelet coefficients at each level are individually tested. After equating some of the wavelet coefficients to zero, the depth bins are reconstructed using the remaining coefficients.

2.4 Depth estimation

In many signal processing applications, ultimate goal is to detect anomalous parts of the received signals, instead of a full characterization of them. This problem is also known as change detection in literature. Simply put, we seek a depth bin (or a set of depth bins) that is statistically different from the depth bins with no buried object. This is a challenging problem as we need to detect the most subtle changes in the GPR data while still maintaining a low false positive rate.[7] In the change detection process, we are limited to nonparametric methods as GPR signals can vary to a great extent under different soil and weather conditions. Without modeling the GPR signals, we try to understand the levels at which abnormal activity occurs. It should be emphasized that the approaches are nonparametric in the sense that noise-free signal is not modeled. As pointed out before, in this study, noise is assumed to have a Gaussian distribution.

2.4.1 Variance method

Obvious solution might be to calculate the variances of each $\mathbf{x}_i$, and seek for deviations from the general trend. More specifically, the depth index at which the variance value is maximum can be taken as the burial depth of the object. In Fig. 3, a sample GPR B-scan, result of background subtraction, and the normalized variances of each depth bin are given.

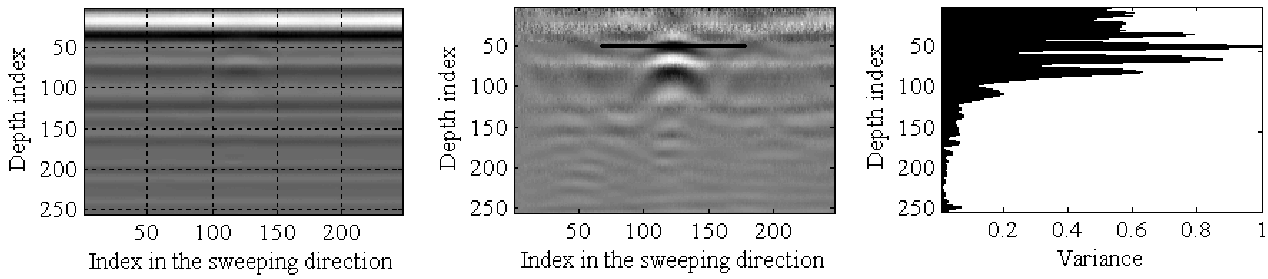

Figure 3. A sample B-scan, result of background subtraction and variances of each depth bin

In this case, the buried object is a TS-50 surrogate mine. It has a diameter of 90 mm and a height of 45 mm. The burial depth is 7 cm. The actual depth of the object is marked with a black stripe in the background subtracted B-scan. It turns out that, variance method can estimate the burial depth of this object. Actually, TS-50 is a challenging mine due to its minimal metal content and relatively small size. For larger surrogate mines, variance method is found out to be satisfactory. However, especially when the detector height is not constant, which is very common in handheld systems, ground bounce cannot be removed by background subtraction. In this case, depth bins inside the ground bounce have large variance values and depth estimates might be wrong. Such an example is given in Fig. 4.

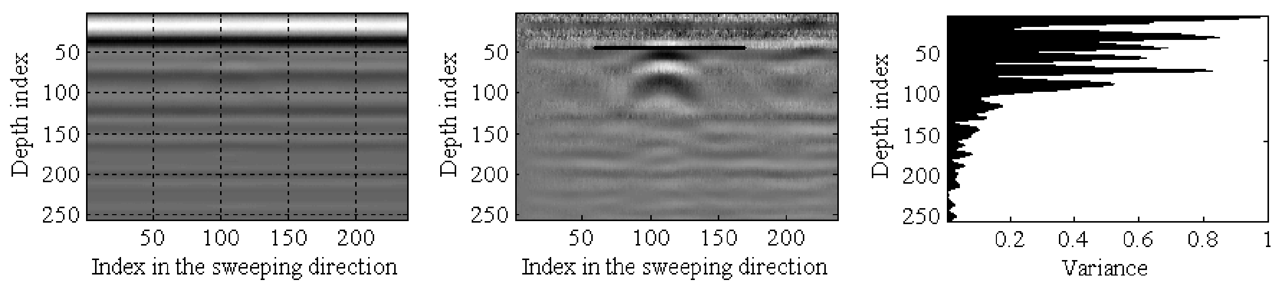

Figure 4. A sample B-scan, result of background subtraction and variances of each depth bin. Maximum variance is observed at a fallacious location in this case.

This example is the B-scan of another TS-50 surrogate mine at the same burial depth, however due to imperfections in data acquisition, ground bounce is more problematic. In this case, we can see that maximum variance value is found to be inside the ground bounce. Hence, depth estimation of the variance method is wrong.

As it turns out, variance method is too superficial for the problem at hand. Next, we use statistical hypothesis tests which are widely exploited to achieve change detection.[8] In change detection approaches with hypothesis testing, possible anomalies form a finite set of hypotheses, which can be denoted as $\mathrm{H} = \{H_i\}_{i=0}^{Q-1}$, where Q is the number of hypotheses. In the depth estimation problem, the number of hypothesis is only 2; absence and presence of a buried object at a given depth bin.

2.4.2 χ^2 goodness-of-fit test

We use χ^2 goodness-of-fit test for each $\mathbf{x}_i$, where the null hypothesis is that, the elements of $\mathbf{x}_i$ are from a normal distribution, where the parameters of the normal distribution are to be estimated from $\mathbf{x}_i$ itself. In the χ^2 test, the statistic which is used to measure the deviation from the hypothesized distribution is roughly related to the frequency diagram constructed from the data set and a corresponding diagram constructed from the hypothesized distribution. The test is performed by grouping the data into k mutually exclusive bins, $A_1, A_2, ..., A_k$. Let O_i be the observed counts for each bin and E_i be the expected counts for each bin. Then, the χ^2 test statistic is

$$\chi^2 = \sum_{i=1}^{N} \frac{(O_i - E_i)^2}{E_i}. \tag{4}$$

The distribution of this statistic converges to χ^2 distribution when the sample size is selected sufficiently large.[9] This statistic is compared with a value obtained from χ^2 tables with ν degrees of freedom. Generally, ν is taken to be $N-1$. However, in our case, mean and variance of the data set are computed from the observed data. To account for these two parameters, ν is taken to be $N-3$. The null hypothesis is rejected if the calculated χ^2 value is greater than the critical value for a given significance level α.

χ^2 goodness-of-fit test requires the expected frequency in each class to be at least 5. Hence, the number of bins one can use is limited.[10] In our implementation, we use 10 bins.

2.4.3 Lilliefors test

The aim of Lilliefors test is the same as the aim of the χ^2 goodness-of-fit test. Again, we are testing whether the data comes from a normal distribution with parameters that are to be estimated from the data itself. In this test, the test statistic is

$$L = \max_{\mathbf{x}_i} \left\{ C\hat{D}F(\mathbf{x}_i) - CDF(\mathbf{x}_i) \right\} \tag{5}$$

where $C\hat{D}F(\mathbf{x}_i)$ is the empirical cumulative distribution function (CDF) estimated from the data vector, and $CDF(\mathbf{x}_i)$ is the normal CDF with mean and standard deviation calculated from $\mathbf{x}_i$. This test statistic is same as the test statistic of Kolmogorov-Smirnov test. The difference between Lilliefors test and Kolmogorov-Smirnov test is that, Kolmogorov-Smirnov test requires the null distribution to be completely specified. On the other hand, in Lilliefors test, parameters of the null distribution are estimated.

A lookup table is used for finding the critical values of the test statistic. This lookup table is generated using Monte Carlo simulations for small sample sizes, because using analytical approximation for small sample sizes is far from being accurate.

2.4.4 Jarque-Bera test

Aim of Jarque-Bera test is the same as the previous hypothesis tests. In Jarque-Bera test, the test statistic is

$$JB = \frac{N}{6} \left(S^2 + \frac{K^2}{4} \right) \tag{6}$$

where N is the number of elements at a depth bin, S is the sample skewness and K is the sample kurtosis. When the sample size is sufficiently large, the distribution of this test statistic converges to a χ^2 distribution with two degrees of freedom.

Again, a lookup table is used to compare this statistic with a critical value. Like Lilliefors test, the lookup table is created using Monte Carlo simulations for greater accuracy.

In all hypothesis tests, each depth bin is tested with the relevant test at the significance level $\alpha = 0.05$, starting from the ground level. If the null hypothesis can be rejected for 20 consecutive depth bins, these bins are marked as target bins. Then, the first bin of these consecutive 20 bins is marked as the burial depth of the object.

3. EXPERIMENTAL RESULTS

This section presents the results of the proposed depth estimation methods. The tests are performed in 3 different pools with 3 different soil types. In all cases, soil is dry and relative static permittivity values of the soil vary between 2.5 and 3. The total number of object signatures is 166. Each object signature consists of 240 A-scans having 256 samples. The buried objects are very diverse, including small plastic anti-personnel surrogate mines, large metal anti-tank surrogate mines and coke cans. The number of each of these objects is given in Table 1.

Table 1. Number of buried objects

Object type	Number of objects
TS-50 surrogate mine	46
VS-50 surrogate mine	22
PMD surrogate mine	20
PMN surrogate mine	20
M-15 surrogate mine	20
M7A2 surrogate mine	17
Coke can	21
TOTAL	**166**

For each object signature, all 4 methods are tested and compared with the ground truth. The ground penetrating radar used in this study has a penetration depth of approximately 50 cm for the tested soil types. Table 2 gives the average depth estimation errors of each method in centimeters for all object types.

Table 2. Average estimation errors of each method (in centimeters)

	χ^2 Test	Lilliefors Test	Jarque-Bera Test	Variance Method
TS-50 surrogate mine	0.132	0.365	0.327	1.329
VS-50 surrogate mine	0.293	0.470	0.320	9.188
PMD surrogate mine	2.734	4.912	3.096	7.139
PMN surrogate mine	0.527	1.094	0.449	9.590
M-15 surrogate mine	1.709	2.373	4.228	6.933
M7A2 surrogate mine	1.287	2.275	4.113	7.893
Coke can	1.200	1.971	1.878	5.422
AVERAGE	**0.958**	**1.655**	**1.728**	**5.931**

As it is evident from Table 2, χ^2 test gives the best overall performance among others. The performances of Lilliefors test and Jarque-Bera test are comparable. Theoretically, these 3 tests all test the same hypothesis. The performance differences show which test statistic is most suitable for depth estimation on GPR data. Variance method seems to have an unacceptably poor performance. Reason of this phenomenon is that, hypothesis tests find the first level at which statistical discrepancies start. On the other hand, maximum variance does not have to be observed at this first level, it can be observed at a depth index which is inside the buried object. Hence, the given depth estimation error is not the true performance indicator of the variance method. To clarify this difference, a sample background subtracted B-scan with depth estimations of all methods is given in Fig. 5.

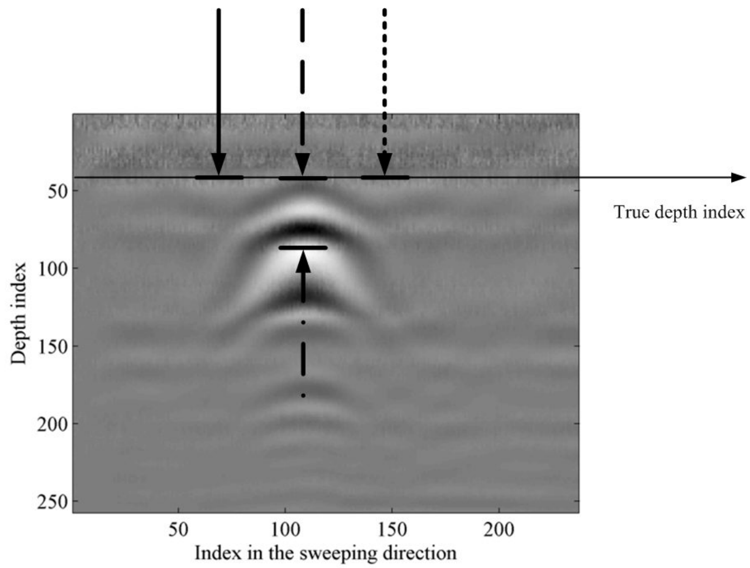

Figure 5. A sample B-scan with depth estimations marked

In this figure, depth estimations of χ^2, Lilliefors and Jarque-Bera tests are marked with solid, dashed and dotted lines respectively. Depth estimation of variance method is marked with dash dotted line. As seen from the figure, results of hypothesis tests overlap, and they are all true. Variance method, on the other hand, locates the center of the buried surrogate mine. This is why numerical results of variance method exhibit a poor performance.

4. CONCLUSION

This paper proposed and compared several burial depth estimation techniques on GPR data. By assuming a Gaussian noise model, Gaussianity test using wavelets and statistical hypothesis tests are performed where the null hypothesis is that, elements of a given depth bin are from a normal distribution with unknown mean and variance. The performances of the proposed methods are compared, and applying χ^2 test on each depth bin is found out to be the most suitable technique for our purposes. Using different objects buried under different types of soil, an average estimation error of 0.95 cm is found for a radar penetration depth of 50 cm for this method.

Future research will focus on the automated selection of the extent of the confidence interval allowed for wavelet coefficients. This will allow the algorithm to estimate the depth of the buried object without any user interaction. Using this depth information, object identification process can be highly improved by using the burial depth as a feature in the classification step.

REFERENCES

[1] Daniels, D. J., [*Ground Penetrating Radar*], IEE Press, London, UK, 2 ed. (2004).

[2] Ho, K. C., Gader, P. D., and Wilson, J. N., "Improving spectral features from GPR by exploring the depth information," *Proc. SPIE* **6217** (2004).

[3] Abujarad, F., Nadim, G., and Omar, A., "Wavelet packets for GPR detection of non-metallic anti-personnel land mines based on higher-order-statistic," *Proceedings of the 3rd International Workshop on Advanced Ground Penetrating Radar*, 21–25 (2005).

[4] Barreiro, R. B., "The discriminating power of wavelets to detect non-Gaussianity in the cosmic microwave background," *Monthly Notices of the Royal Astronomical Society* **327**, 813–828(16) (2001).

[5] Mukherjee, P., "Do wavelets really detect non-Gaussianity in the 4-year COBE data?," *Monthly Notices of the Royal Astronomical Society* **318**, 1157–1163(7) (2000).

[6] Kim, T.-H. and White, H., "On more robust estimation of skewness and kurtosis," *Finance Research Letters* **1**(1), 56–73 (2004).
[7] Song, X., Wu, M., Jermaine, C., and Ranka, S., "Statistical change detection for multi-dimensional data," *Proceedings of the 13th International Conference on Knowledge Discovery and Data Mining*, 667–676 (2007).
[8] Frakt, A. B., Willsky, A. S., and Karl, W. C., "Multiscale hypothesis testing with application to anomaly characterization from tomographic projections," *International Conference on Image Processing* **1**, 705–708 (1996).
[9] Soong, T. T., [*Fundamentals of probability and statistics for engineers*], John Wiley & Sons, West Sussex, England (2004).
[10] Kanji, G. K., [*100 statistical tests*], Sage Publications, London, England, 3 ed. (2006).